NANO LETTERS

pubs.acs.org/NanoLett

Letter

Orientational Ordering in Nano-confined Polar Liquids

Karina Pivnic,[⊥] J. Pedro de Souza,[⊥] Alexei A. Kornyshev, Michael Urbakh, and Martin Z. Bazant*

Cite This: https://doi.org/10.1021/acs.nanolett.3c00927

Read Online

ACCESS | Metrics & More | Article Recommendations | Supporting Information

ABSTRACT: Water and other polar liquids exhibit nanoscale structuring near charged interfaces. When a polar liquid is confined between two charged surfaces, the interfacial solvent layers begin to overlap, resulting in solvation forces. Here, we perform molecular dynamics simulations of polar liquids with different dielectric constants and molecular shapes and sizes confined between charged surfaces, demonstrating strong orientational ordering in the nanoconfined liquids. To rationalize the observed structures, we apply a coarse-grained continuum theory that captures the orientational ordering and solvation forces of those liquids. Our findings reveal the subtle behavior of different nanoconfined polar liquids and establish a simple law for the decay length of the interfacial orientations of the solvents, which depends on their molecular size and polarity. These insights shed light on the nature of solvation forces, which are important in colloid and membrane science, scanning probe microscopy, and nano-electrochemistry.

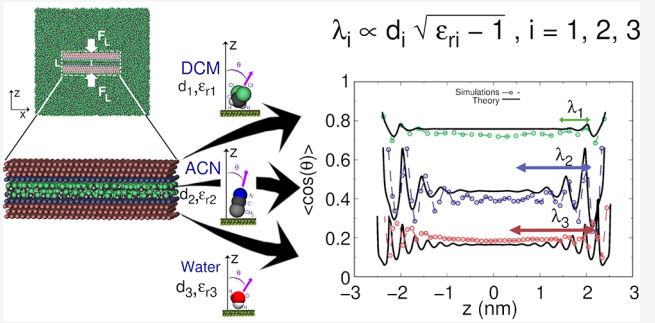

KEYWORDS: *Nano-confinement, polar liquids, orientational ordering, solvation forces, dielectric theory, molecular dynamics simulations*

The interfacial structuring of water and other polar liquids fundamentally determines the physical, biophysical, and electrochemical interfacial properties in numerous observable phenomena in science and engineering.[1−4] These include the interactions of biopolymers such as DNA or proteins,[5,6] transport through biological or synthetic membrane pores,[7] interactions within industrial or engineered colloids such as cement pastes,[8] and electrochemical reactions and capacitive charge storage,[9−11] among many others. In each of these processes, liquid molecules exhibit preferential orientation due to the liquid-substrate interaction and charge on the bounding solid surfaces, leading to unique liquid properties near the interface.

Currently, there is a lack of understanding of the interfacial ordering in polar liquids, especially as compared to our understanding of charge screening in dilute electrolytes, in which the charge, due to counterions and co-ions near a charged surface, generally decays over a well-known Gouy−Chapman or Debye length.[12−14] Very often, and even now, the solvent in such systems is described within the primitive model, characterized by a macroscopic dielectric constant. But it is commonly understood that such an approach breaks down near interfaces or in strong confinement. Indeed, numerous simulations[15−25] have shown that there is charge layering due to the orientational ordering of water within ∼1 nm of an interface, consistent with the experimentally observed structuring of interfacial water.[26−30] Although these molecules possess no net charge, the local regions of positive and negative bound charge on the molecules cooperatively form layers of alternating charge at the interface as the molecules are oriented by an applied electric field. This has strong implications for the local dielectric properties and thus the behavior of the fluid under confinement.[31] Nevertheless, the orientational structuring of nanoconfined polar liquids beyond solely water still remains poorly understood.

Recently, de Souza et al. developed a continuum theory[31] that describes the orientational ordering by representing the liquid molecules as dipolar spherical shells. While the theoretical predictions are generally consistent with previous simulation results,[17] nonlocal dielectric theories,[32−41] and integral equation approaches,[42−51] the dipolar shell theory predicts a simple relationship between the orientational ordering and the physical properties of the liquid. In particular, the effective polar liquid molecular diameter, d, and the bulk dielectric constant, ϵ_r, determine the oscillatory decay of interfacial dipole orientations. In linear response, the model predicts that the nonlocal dielectric response involves decaying orientations of polar liquids over a "solvation length", λ, given by

$$\lambda = \alpha d\sqrt{\epsilon_r - 1} \tag{1}$$

Received: March 10, 2023
Revised: May 22, 2023

with oscillations on the order of a single molecular diameter, where the proportionality factor α is an $O(1)$ constant.

In the present work, we use molecular dynamics (MD) simulations to study the orientational ordering of three polar liquids - dichloromethane, acetonitrile, and water. Our aim is to identify common features in the orientational ordering for this set of "realistic" liquids and to probe the applicability of the dipolar shell theory presented above in relating these features to the physical properties of the liquid. The chosen liquids possess varying dielectric constants, molecular shapes, sizes, and densities characterized by the different force-fields that are used for the different tested molecules. The liquids are confined between two oppositely charged surfaces, with varying extents of confinement (Figure 1a). The case of

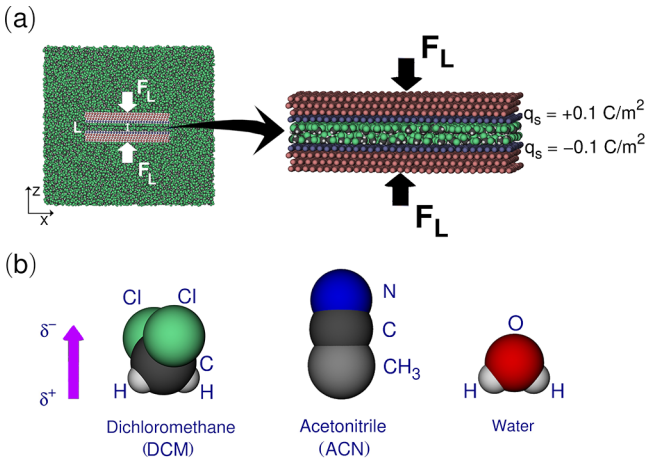

Figure 1. Simulation schematic. (a) The polar liquids are confined between two surfaces with separation distance, L, under the application of normal forces, F_L. The surfaces are oppositely charged, and the polar liquid between them orients in response to this polarization. (b) The three molecules studied here, with dipole moment oriented upward. The molecules are dichloromethane, acetonitrile, and water.

oppositely charged surfaces is easier to study in molecular simulations, as it maintains electroneutrality in the system, whereas it is not principle for the theory. However, the insights from this study can easily be extended to more general cases. Essentially, by squeezing-out the liquid confined between the surfaces, we determine their structural solvation forces and orientational ordering at nanometric surface separations.

Overall, the simulation results demonstrate that for the three polar liquids, the orientational ordering near a charged surface displays oscillations which extend over a solvation length, a quantity that increases in its extent with increasing liquid polarity and molecular size, consistent with the solvation length prediction in eq 1. When the surface separation is comparable to the solvation length, the oscillatory structures overlap to form coherent patterns between the surfaces that correspond to strong solvation forces. Furthermore, while we find that the dipolar shell theory, due to its coarse-graining assumptions, is limited in capturing all the detailed structures in density and structural forces, its power lies in its ability to analtyically predict a set of key features of the orientational ordering near the interface and in confinement in a single, consistent theoretical framework.

In Figure 1b, we show the three polar molecules under investigation. Depending on the liquid, the respective molecules are simulated using different force-fields. The dichloromethane molecule is simulated using OPLS-AA force field parameters,[52,53] the acetonitrile is simulated using a coarse-grained model reported in ref 54, and the water molecules are represented using the TIP3P model.[55] The force-fields chosen to describe each liquid are well-established force-fields that reproduce experimental bulk properties. Particularly, the bulk densities of the fluids are computed at T = 300 K and P = 1 bar to be c_d = 15.7 M for dichloromethane, c_d = 19.1 M for acetonitrile, and c_d = 55 M for water, and the bulk permittivity of each liquid is approximately $\epsilon_r \approx 9$ for dichloromethane, $\epsilon_r \approx 39$ for acetonitrile, and $\epsilon_r \approx 100$ for TIP3P water. Despite having specific molecular shapes, for the purposes of comparison to eq 1 and the full nonlinear theory,[31] we assign a single structural parameter to the molecules - an effective spherical diameter, d. This quantity is derived from the first peak found in the center-of-mass radial distribution function computed for the respective bulk liquid. These effective sizes are found to be as follows: d = 0.38 nm for dichloromethane, d = 0.424 nm for acetonitrile, and d = 0.285 nm for TIP3P water. Essentially, due to their different effective sizes and bulk dielectric constants, the particular choice of these liquids therefore allow us to sample various values of effective solvation lengths.

We immerse two parallel plates in the $x-y$ plane in a given bulk liquid consisting of any of the polar molecules mentioned above. We consider flat surfaces comprising LJ spheres, with the FCC (111) plane in contact with the confined liquid, and a lattice parameter corresponding to "gold".[56] The solid surfaces, which are immersed in the liquid, are of finite size in the x and z directions. The solid surfaces are arranged to create two regions of the fluid, bulk and confined, to facilitate studies of the properties of the confined thin liquid films, which are in equilibrium with a surrounding bulk liquid. Finite size effects have been considered in our work. However, to circumvent such effects, alternative methodologies which employ thermodynamic extrapolation techniques can be used[58] To study the orientational ordering of the confined fluid in response to an applied electric field, while maintaining the overall electroneutrality of the system, we assign constant, opposite charges on the surfaces of the plates. The absolute surface charge density on each plate was taken to be $|q_s| = 0.1$ C/m^2.

To compute the nanoconfined orientational profiles and simulate solvation forces, the systems are set up as follows. The plates are positioned at an initial distance, L, from each other, in the normal direction, where typically $L \approx 5.5$ nm. The plates are then pushed toward one another, dynamically, varying the separation distance to generate the solvation forces, F_L, or equivalently, pressure profiles. By using this method, the whole range of interplate distances can be accessed, reaching both stable and unstable states, and the full pressure profiles are produced.[56,57] Further, we compute the time-averaged orientation profiles of the liquid in the confined gap from an additional set of simulations, in which we apply identical constant normal loads to both plates, until they reach their equilibrium positions.[56] At a fixed equilibrium separation distance of the plates, L, which corresponds to a stable state distance found in the pressure profiles, we compute the orientation profiles in the confined region. Generally, the molecular orientation profiles are calculated as the laterally $(x-y)$ averaged angle between the direction of the dipole moment of the molecules and the normal axis, z (see insets of Figure 2), and plotted as a function of this axis. It should be

https://doi.org/10.1021/acs.nanolett.3c00927
Nano Lett. XXXX, XXX, XXX−XXX

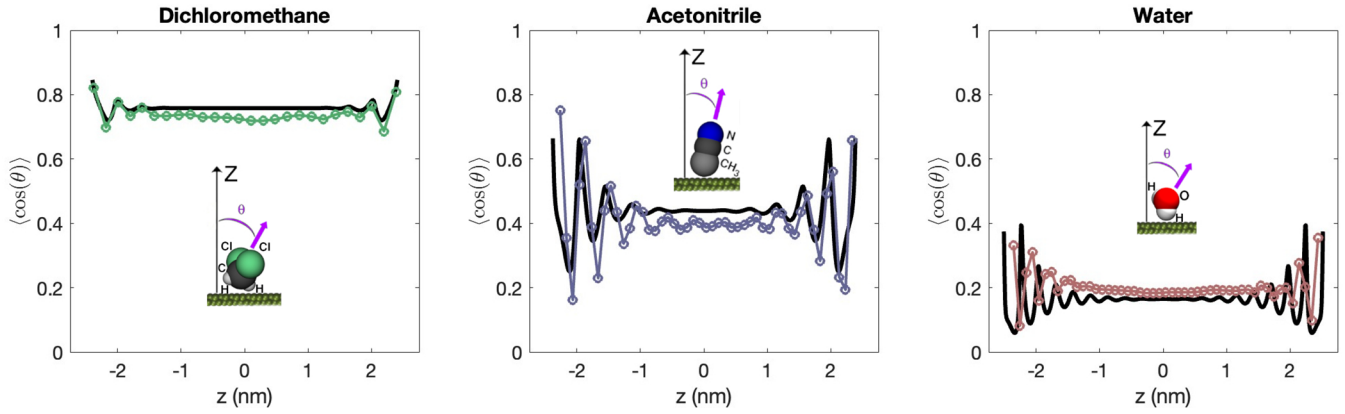

Figure 2. Liquid molecular orientation profiles for large surface separations. The simulation is shown with colored symbols. The theory predictions are shown with black solid lines. The profiles of $\langle \cos(\theta) \rangle$ display decaying oscillations as a function of z until they reach a constant value in the center of the gap ($z = 0$). The two surfaces have equal but opposite surface charge density of $q_s = \pm 0.1$ C/m^2, and the separation distances of the two surfaces are around 5.5 nm for all the liquids.

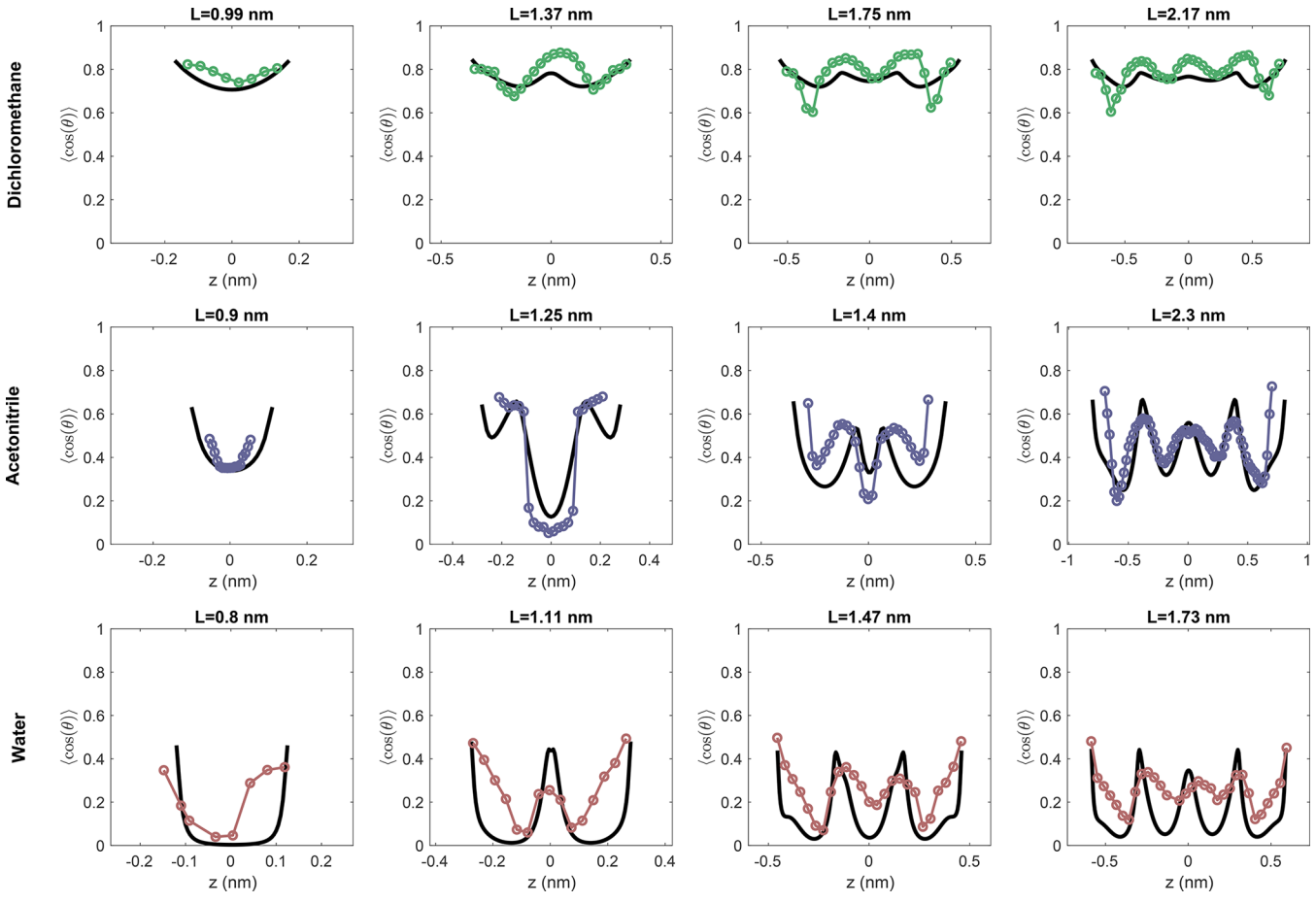

Figure 3. Confined liquid molecular orientation profiles with solvation layering overlap. The simulation is shown with colored symbols. The theory predictions are shown with black solid lines. The profiles of $\langle \cos(\theta) \rangle$ include oscillatory structures that emanate from each surface and they overlap under confinement. The center of the gap is at $z = 0$. The two confining surfaces have equal but opposite surface charge density of $q_s = \pm 0.1$ C/m^2, and the separation distance of the two surfaces, L, varies based on the title of each subplot.

noted that from these equilibrium simulations, having several fixed separation distances for different applied normal forces, a discontinuous force profile can also be produced. We find that this force profile is comparable to the continuous force profile obtained from the dynamic simulations that justifies their ustilization. It should also be noted that at strong confinements, where strongly surface-bound water needs to be removed, it was previously found that shearing velocities of 0.001 m/s are needed to reach the quasi static limit for ultraconfined water.[59] Further explanations and details on the simulation setup, methods and theoretical calculations can be found in the Supporting Information (SI).

As we present the simulation results, it is useful to contrast them to a more familiar example: the ideal parallel plate

https://doi.org/10.1021/acs.nanolett.3c00927
Nano Lett. XXXX, XXX, XXX−XXX

capacitor with constant dielectric constant of the medium between the plates. In this system, the electric field would be a constant between the two charged surfaces, and all embedded dipoles would have the same orientation. However, as we can clearly see in Figure 2, the simulation predictions for each liquid (colored symbols) show oscillations in the orientations of the liquids near the interfaces. These orientational oscillations correspond to the charge layering near the interfaces which are not captured by standard dielectric theories of the ideal parallel plate capacitor. The orientational ordering is, however, closely captured by the dipolar shell theory (solid black curves) in magnitude, wavelength, and extent.

At the separation distance of $L \approx 5.5$ nm presented in Figure 2, the oscillations of the orientation angle in all liquids consistently decay to a constant in the center of the gap. Clearly, for all polar liquids studied here, the decay in oscillations closely mirrors the prediction of the solvation length given by the dipolar shell theory presented in eq 1, where $\alpha = 1/\sqrt{6}$, as derived in the SI. The least polar fluid, dichloromethane, has a predicted solvation length of $\lambda \approx 0.4$ nm, while acetonitrile has a solvation length of $\lambda \approx 1.1$ nm, and the TIP3P water has a solvation length of $\lambda \approx 1.2$ nm. In the simulations, slight asymmetries in the orientation profiles at oppositly charged surfaces are observed, due to the asymmetric size and charge distributions in the molecules. In Figure S5 in the SI, we present results of additional simulations which use a reference system of spherical liquid molecules utilizing the Stockmayer potential. Each liquid possesses its own dielectric constant ϵ_r and a fixed molecular diameter d. These results provide further support and validate the scaling of the solvation layering.

At narrow confinements, the orientational ordering of the polar liquids emanating from each surface can constructively or destructively interfere with each other. As shown in Figure 3, the extent of confinement can strongly influence the orientational ordering of the polar liquid. Again, the dipolar shell theory can capture the layered structures even in narrow confinement, including orientations that activate the nonlinear, nonlocal dielectric response of the liquid. Clearly, there are some discrepancies between the simulation and the theory. For dichloromehtane, the oscillations are stronger in the simulation than they appear in the theory. On the other hand, for water, the oscillations appear to be too strong in the theory. Still, the theory consistently predicts the main features observed in the simulations for the orientational ordering even for these liquids under extreme confinement.

Finally, in Figure 4, we present a comparison of the predicted disjoining pressure profiles between two oppositely charged surfaces for varying surface separations in the three liquids. We find that the theory generally under-predicts the magnitudes of the oscillatory structural forces compared to the simulations, particularly at small separation distances, and for the molecules with more asymmetric shapes - dichloromethane and acetonitrile. In addition, for acetonitrile, there are even discrepancies in the predicted peak positions of the stable and unstable states. These discrepancies appear to occur despite the agreements in the orientation profiles for both of these liquids. On the other hand, the theoretical predictions of the structural forces for the TIP3P water are reasonably matched to the simulations, even for the smallest separation distances.

The discrepancy between the disjoining pressures in the simulation and the theory can mainly be attributed to the

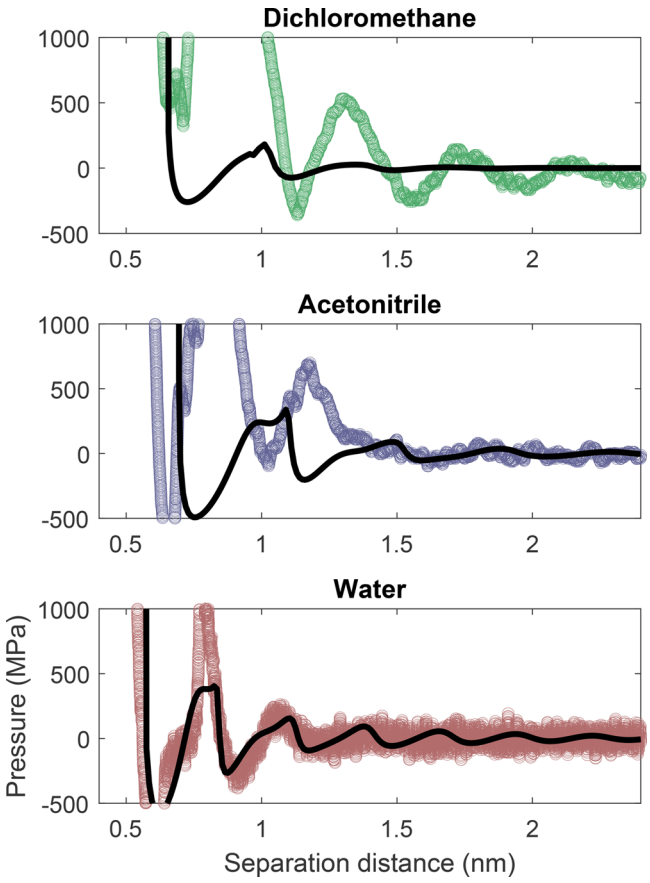

Figure 4. Disjoining pressure predictions for polar liquids between two oppositely charged surfaces as a function of surface separation distance. The colored symbols correspond to the pressures calculated from the MD simulations, while the black solid lines correspond to the theoretical predictions.

discrepancy between the theoretical and simulated density profiles of the liquids, especially in strong confinement as shown in Figures S2−S4. Primarily, these density discrepancies occur due to the fact that the dipolar shell theory represents the molecules of complicated shape and "soft" interaction potentials as effective hard spheres. Clearly, this hard sphere assumption is responsible for the poor performance of the theory to reproduce the structural forces at close separations, particularly for acetonitrile and dichloromethane. While direct surface interactions between the soft surfaces in the simulation may also play a role near contact, it is the packing of the liquids that leads to irregular periodicity in the force profiles. The structural features of the density in the first few molecular layers are not captured by the solvation length predictions given by eq 1, and therefore, the decay of forces in the most extreme confinements are not accurately captured. In the SI, we demonstrate that the liquids with molecules whose shape is represented with spherical, but soft Stockmayer liquids exhibit better qualitative agreement between solvation forces predicted theoretically and in simulations.

It may appear that, for all liquids studied here, the orientational ordering at charged surfaces can be primarily captured by the analytical theory with only two material parameters, the bulk dielectric constant and the molecular size. In reality, however, the intermolecular forces are an intrinsic part of the model, and they determine all the correlations in these liquids, as well as in the end the values of the

https://doi.org/10.1021/acs.nanolett.3c00927
Nano Lett. XXXX, XXX, XXX−XXX

macroscopic dielectric constants. Still, it is remarkable that the solvation lengths contain only those two parameters. Thus, the dipole−dipole correlations only participate in setting the dielectric response of the liquid, while the orientational ordering is governed by a mean-field response to the electric field that determines solvation layering emanating from a charged interface.

While our simulations and model are focused on pure polar liquids, most practical systems include some amount of dissolved salts. The simulations and theory could be naturally extended to describe electrolyte solutions or mixtures of liquids, including systems with size asymmetry. In these cases, oscillatory patterns may be sensitive to the coherency of the solvent and ionic charge ordering, depending on the size asymmetry and specific interactions of the ions with the solvent and surface. Further, the orientational ordering of solvent may affect electrochemical behavior out of equilibrium, although one may need to consider the orientational frustration and altered mobility of the interfacial liquid.

To summarize and conclude, when polar liquids come in contact with a charged solid surface, they form orientationally ordered interfacial structures. Due to the charge distributions in the molecule and its finite size, there are oscillations in the orientation distributions near the interfaces. When two surfaces approach each other, the charge distributions in the embedded liquid merge, leading to coherent oscillations and solvation interactions based on the orientational ordering of the solvent.

These features have been demonstrated here for three "realistic" polar liquids using MD simulations. Furthermore, applying a dipolar shell theory,[31] we have shown that two physical parameters, the effective polar liquid molecular diameter, d, and the bulk dielectric constant, ϵ_r, determine the orientational ordering in confined liquids. Although the theory is able to capture the oscillatory decay of interfacial molecular orientations, it cannot quantitatively describe the structural forces for very asymmetrically sized molecules at the smallest separation distances. While we expect the orientational structuring over the solvation length to be a universal feature in dielectric screening by polar liquids, other surface-specific interactions may also participate in the liquid's interfacial structure. In fact, specific, orientation-dependent solvent-surface interactions can further bias the solvent polarization on the surface.

It has also recently been shown that the smearing of the surface (and of the boundary condition) may dramatically affect the polarization profiles;[60] a strong and nontrivial effect is also expected to come from the lateral inhomogeneity of the surfaces.[61] In the present study we have considered ideally smooth, laterally homogeneous, and sharp surfaces, whereas in reality in many systems they are not as such. This simulation and theoretical study, however, describes the ideal reference frame, on top of which the influence of those more complex features could be incorporated. A more involved theoretical approach would be necessary to describe the orientation-dependent packing of the molecules when they have complicated shapes or specific interactions with the confining surfaces beyond the response to their electric charge.

Nevertheless, the evidence from the molecular simulations presented here uncovers simple trends in the solvation of surfaces by liquids. These findings may be integrated beyond just a nanoconfined liquid capacitor studied here, to systems with nonzero ionic concentrations and reactive surfaces in which the local solvent orientations affect surface forces and electrochemical driving forces for reactions. In practice, the solvation length predictions could be used to rationalize measurements of colloidal interactions, develop strategies for colloidal stabilization, or characterize the nanoscopic electrochemical properties of solid−liquid interfaces.

■ ASSOCIATED CONTENT

Supporting Information

The Supporting Information is available free of charge at https://pubs.acs.org/doi/10.1021/acs.nanolett.3c00927.

Additional simulation and theoretical details and results, solvation length interpretation, density variations in confined polar liquids, simulations with a Stockmayer liquid model (PDF)

■ AUTHOR INFORMATION

Corresponding Author

Martin Z. Bazant − *Department of Chemical Engineering, Massachusetts Institute of Technology, Cambridge, Massachusetts 02139, United States; Department of Mathematics, Massachusetts Institute of Technology, Cambridge, Massachusetts 02139, United States;* orcid.org/0000-0002-8200-4501; Email: bazant@mit.edu

Authors

Karina Pivnic − *School of Chemistry, The Sackler Center for Computational Molecular and Materials Science, Tel Aviv University, Tel Aviv 6997801, Israel*

J. Pedro de Souza − *Department of Chemical Engineering, Massachusetts Institute of Technology, Cambridge, Massachusetts 02139, United States;* orcid.org/0000-0003-3634-4991

Alexei A. Kornyshev − *Department of Chemistry, Molecular Sciences Research Hub, Imperial College London, W12 0BZ 2AZ London, United Kingdom; Thomas Young Centre for Theory and Simulation of Materials, Imperial College London, London SW7 2AZ, United Kingdom;* orcid.org/0000-0002-3157-8791

Michael Urbakh − *School of Chemistry, The Sackler Center for Computational Molecular and Materials Science, Tel Aviv University, Tel Aviv 6997801, Israel;* orcid.org/0000-0002-3959-5414

Complete contact information is available at: https://pubs.acs.org/10.1021/acs.nanolett.3c00927

Author Contributions

[⊥]K.P. and J.P.D. contributed equally to this work.

Notes

The authors declare no competing financial interest.

■ ACKNOWLEDGMENTS

K.P. and M.U. acknowledge the financial support of the Israel Science Foundation under grant number 1141/18. J.P.D. and M.Z.B. acknowledge partial support from the Center for Enhanced Nanofluidic Transport, an Energy Frontier Research Center funded by the U.S. Department of Energy, Office of Science, Basic Energy Sciences under Award No. DE-SC0019112. J.P.D. also acknowledges support from the National Science Foundation Graduate Research Fellowship under Award No. 1122374. AAK uses this chance to acknowledge the useful discussions and joint work on a

https://doi.org/10.1021/acs.nanolett.3c00927
Nano Lett. XXXX, XXX, XXX−XXX

related topic with Helene Berthoumieux (Sorbonne University) and Jonathan Hedley (Imperial College).

REFERENCES

(1) Bard, A. J.; Faulkner, L. R. *Electrochemical Methods: Fundamentals and Applications*; Wiley: New York, 2001.
(2) Bockris, J. O.; Reddy, A. K. N.; Gamboa-Aldeco, M. *Modern Electrochemistry: Fundamentals of Electrodics*; Kluwer Academic Publishers: New York, 2000.
(3) Björneholm, O.; Hansen, M. H.; Hodgson, A.; Liu, L.-M.; Limmer, D. T.; Michaelides, A.; Pedevilla, P.; Rossmeisl, J.; Shen, H.; Tocci, G.; et al. Water at interfaces. *Chem. Rev.* **2016**, *116*, 7698−7726.
(4) Schmickler, W.; Santos, E. *Interfacial electrochemistry*; Springer Science & Business Media, 2010.
(5) Israelachvili, J.; Wennerström, H. Role of hydration and water structure in biological and colloidal interactions. *Nature* **1996**, *379*, 219−225.
(6) Kornyshev, A.; Leikin, S. Theory of interaction between helical molecules. *J. Chem. Phys.* **1997**, *107*, 3656−3674.
(7) Tunuguntla, R. H.; Henley, R. Y.; Yao, Y.-C.; Pham, T. A.; Wanunu, M.; Noy, A. Enhanced water permeability and tunable ion selectivity in subnanometer carbon nanotube porins. *Science* **2017**, *357*, 792−796.
(8) Misra, R. P.; de Souza, J. P.; Blankschtein, D.; Bazant, M. Z. Theory of surface forces in multivalent electrolytes. *Langmuir* **2019**, *35*, 11550−11565.
(9) Bockris, J.; Devanathan, M.; Müller, K. *Electrochemistry*; Elsevier, 1965; pp 832−863.
(10) Gonella, G.; Backus, E. H.; Nagata, Y.; Bonthuis, D. J.; Loche, P.; Schlaich, A.; Netz, R. R.; Kühnle, A.; McCrum, I. T.; Koper, M.; et al. Water at charged interfaces. *Nature Reviews Chemistry* **2021**, *5*, 466−485.
(11) Santos, E.; Schmickler, W. Models of electron transfer at different electrode materials. *Chem. Rev.* **2022**, *122*, 10581−10598.
(12) Israelachvili, J. N. *Intermolecular and Surface Forces*; Academic Press, 2011.
(13) Honig, B.; Nicholls, A. Classical electrostatics in biology and chemistry. *Science* **1995**, *268*, 1144−1149.
(14) Andelman, D. Introduction to electrostatics in soft and biological matter. *Soft Condensed Matter Physics in Molecular and Cell Biology* **2006**, *59*, 97−118.
(15) Janeček, J.; Netz, R. R. Interfacial water at hydrophobic and hydrophilic surfaces: Depletion versus adsorption. *Langmuir* **2007**, *23*, 8417−8429.
(16) Bonthuis, D. J.; Gekle, S.; Netz, R. R. Dielectric profile of interfacial water and its effect on double-layer capacitance. *Physical review letters* **2011**, *107*, 166102.
(17) Bonthuis, D. J.; Gekle, S.; Netz, R. R. Profile of the static permittivity tensor of water at interfaces: Consequences for capacitance, hydration interaction and ion adsorption. *Langmuir* **2012**, *28*, 7679−7694.
(18) Bonthuis, D. J.; Netz, R. R. Beyond the continuum: How molecular solvent structure affects electrostatics and hydrodynamics at solid−electrolyte interfaces. *J. Phys. Chem. B* **2013**, *117*, 11397−11413.
(19) Mashayak, S.; Aluru, N. Langevin-Poisson-EQT: A dipolar solvent based quasi-continuum approach for electric double layers. *J. Chem. Phys.* **2017**, *146*, 044108.
(20) Olivieri, J.-F.; Hynes, J. T.; Laage, D. Confined Water's Dielectric Constant Reduction Is Due to the Surrounding Low Dielectric Media and Not to Interfacial Molecular Ordering. *J. Phys. Chem. Lett.* **2021**, *12*, 4319−4326.
(21) Deißenbeck, F.; Freysoldt, C.; Todorova, M.; Neugebauer, J.; Wippermann, S. Dielectric Properties of Nanoconfined Water: A Canonical Thermopotentiostat Approach. *Phys. Rev. Lett.* **2021**, *126*, 136803.
(22) Ruiz-Barragan, S.; Muñoz-Santiburcio, D.; Körning, S.; Marx, D. Quantifying anisotropic dielectric response properties of nanoconfined water within graphene slit pores. *Phys. Chem. Chem. Phys.* **2020**, *22*, 10833−10837.
(23) Motevaselian, M. H.; Aluru, N. R. Universal reduction in dielectric response of confined fluids. *ACS Nano* **2020**, *14*, 12761−12770.
(24) Motevaselian, M.; Mashayak, S.; Aluru, N. Extended coarse-grained dipole model for polar liquids: Application to bulk and confined water. *Phys. Rev. E* **2018**, *98*, 052135.
(25) Scalfi, L.; Dufils, T.; Reeves, K. G.; Rotenberg, B.; Salanne, M. A semiclassical Thomas-Fermi model to tune the metallicity of electrodes in molecular simulations. *J. Chem. Phys.* **2020**, *153*, 174704.
(26) Chiang, K.-Y.; Seki, T.; Yu, C.-C.; Ohto, T.; Hunger, J.; Bonn, M.; Nagata, Y. The dielectric function profile across the water interface through surface-specific vibrational spectroscopy and simulations. *Proc. Natl. Acad. Sci. U. S. A.* **2022**, *119*, e2204156119.
(27) Fenter, P.; Sturchio, N. C. Mineral−water interfacial structures revealed by synchrotron X-ray scattering. *Prog. Surf. Sci.* **2004**, *77*, 171−258.
(28) Leikin, S.; Parsegian, V. A.; Rau, D. C.; Rand, R. P. Hydration forces. *Annu. Rev. Phys. Chem.* **1993**, *44*, 369−395.
(29) Johnson, G.; Lecchini, S.; Smith, E.; Clifford, J.; Pethica, B. Role of water structure in the interpretation of colloid stability. *Discuss. Faraday Soc.* **1966**, *42*, 120−133.
(30) Israelachvili, J. N.; Pashley, R. M. Molecular layering of water at surfaces and origin of repulsive hydration forces. *Nature* **1983**, *306*, 249−250.
(31) de Souza, J.; Kornyshev, A. A.; Bazant, M. Z. Polar liquids at charged interfaces: A dipolar shell theory. *J. Chem. Phys.* **2022**, *156*, 244705.
(32) Kornyshev, A.; Schmickler, W.; Vorotyntsev, M. Nonlocal electrostatic approach to the problem of a double layer at a metal-electrolyte interface. *Phys. Rev. B* **1982**, *25*, 5244.
(33) Kornyshev, A. A. Non-local dielectric response of a polar solvent and Debye screening in ionic solution. *Journal of the Chemical Society, Faraday Transactions 2: Molecular and Chemical Physics* **1983**, *79*, 651−661.
(34) Belaya, M.; Feigel'Man, M.; Levadny, V. Hydration forces as a result of non-local water polarizability. *Chem. Phys. Lett.* **1986**, *126*, 361−364.
(35) Bopp, P. A.; Kornyshev, A. A.; Sutmann, G. Static nonlocal dielectric function of liquid water. *Phys. Rev. Lett.* **1996**, *76*, 1280.
(36) Kornyshev, A. A.; Sutmann, G. The shape of the nonlocal dielectric function of polar liquids and the implications for thermodynamic properties of electrolytes: A comparative study. *J. Chem. Phys.* **1996**, *104*, 1524−1544.
(37) Kornyshev, A. A.; Sutmann, G. Nonlocal dielectric saturation in liquid water. *Phys. Rev. Lett.* **1997**, *79*, 3435.
(38) Bopp, P. A.; Kornyshev, A. A.; Sutmann, G. Frequency and wave-vector dependent dielectric function of water: Collective modes and relaxation spectra. *J. Chem. Phys.* **1998**, *109*, 1939−1958.
(39) Levy, A.; Bazant, M.; Kornyshev, A. Ionic activity in concentrated electrolytes: Solvent structure effect revisited. *Chem. Phys. Lett.* **2020**, *738*, 136915.
(40) Monet, G.; Bresme, F.; Kornyshev, A.; Berthoumieux, H. Nonlocal dielectric response of water in nanoconfinement. *Phys. Rev. Lett.* **2021**, *126*, 216001.
(41) Blossey, R.; Podgornik, R. Field theory of structured liquid dielectrics. *Physical Review Research* **2022**, *4*, 023033.
(42) Chandler, D.; Andersen, H. C. Optimized cluster expansions for classical fluids. II. Theory of molecular liquids. *J. Chem. Phys.* **1972**, *57*, 1930−1937.
(43) Hirata, F.; Pettitt, B. M.; Rossky, P. J. Application of an extended RISM equation to dipolar and quadrupolar fluids. *J. Chem. Phys.* **1982**, *77*, 509−520.
(44) Pettitt, B. M.; Rossky, P. J. Integral equation predictions of liquid state structure for waterlike intermolecular potentials. *J. Chem. Phys.* **1982**, *77*, 1451−1457.

https://doi.org/10.1021/acs.nanolett.3c00927
Nano Lett. XXXX, XXX, XXX−XXX

(45) Ikeguchi, M.; Doi, J. Direct numerical solution of the Ornstein−Zernike integral equation and spatial distribution of water around hydrophobic molecules. *J. Chem. Phys.* **1995**, *103*, 5011−5017.
(46) Lue, L.; Blankschtein, D. Application of integral equation theories to predict the structure, thermodynamics, and phase behavior of water. *J. Chem. Phys.* **1995**, *102*, 5427−5437.
(47) Beglov, D.; Roux, B. An integral equation to describe the solvation of polar molecules in liquid water. *J. Phys. Chem. B* **1997**, *101*, 7821−7826.
(48) Trokhymchuk, A.; Henderson, D.; Wasan, D. T. A molecular theory of the hydration force in an electrolyte solution. *J. Colloid Interface Sci.* **1999**, *210*, 320−331.
(49) Du, Q.; Beglov, D.; Roux, B. Solvation free energy of polar and nonpolar molecules in water: An extended interaction site integral equation theory in three dimensions. *J. Phys. Chem. B* **2000**, *104*, 796−805.
(50) Fedorov, M. V.; Kornyshev, A. A. Unravelling the solvent response to neutral and charged solutes. *Mol. Phys.* **2007**, *105*, 1−16.
(51) Wu, J.; Li, Z. Density-functional theory for complex fluids. *Annu. Rev. Phys. Chem.* **2007**, *58*, 85−112.
(52) Caleman, C.; Van Maaren, P. J.; Hong, M.; Hub, J. S.; Costa, L. T.; Van Der Spoel, D. Force field benchmark of organic liquids: density, enthalpy of vaporization, heat capacities, surface tension, isothermal compressibility, volumetric expansion coefficient, and dielectric constant. *J. Chem. Theory Comput.* **2012**, *8*, 61−74.
(53) Liu, Z.; Timmermann, J.; Reuter, K.; Scheurer, C. Benchmarks and dielectric constants for reparametrized OPLS and polarizable force field models of chlorinated hydrocarbons. *J. Phys. Chem. B* **2018**, *122*, 770−779.
(54) Edwards, D. M.; Madden, P. A.; McDonald, I. R. A computer simulation study of the dielectric properties of a model of methyl cyanide: I. The rigid dipole case. *Mol. Phys.* **1984**, *51*, 1141−1161.
(55) Mark, P.; Nilsson, L. Structure and dynamics of the TIP3P, SPC, and SPC/E water models at 298 K. *J. Phys. Chem. A* **2001**, *105*, 9954−9960.
(56) Pivnic, K.; Bresme, F.; Kornyshev, A. A.; Urbakh, M. Structural forces in mixtures of ionic liquids with organic solvents. *Langmuir* **2019**, *35*, 15410−15420.
(57) Capozza, R.; Vanossi, A.; Benassi, A.; Tosatti, E. Squeezout phenomena and boundary layer formation of a model ionic liquid under confinement and charging. *J. Chem. Phys.* **2015**, *142*, 064707.
(58) Kanduc, M.; Schlaich, A.; Schneck, E.; Netz, R. R. Water-mediated interactions between hydrophilic and hydrophobic surfaces. *Langmuir* **2016**, *32*, 8767−8782.
(59) Schlaich, A.; Kappler, J.; Netz, R. R. Hydration friction in nanoconfinement: From bulk via interfacial to dry friction. *Nano Lett.* **2017**, *17*, 5969−5976.
(60) Hedley, J. G.; Berthoumieux, H.; Kornyshev, A. A. The Dramatic Effect of Water Structure on Hydration Forces and the Electrical Double Layer. *J. Phys. Chem. C* **2023**, *127*, 8429−8447.
(61) Kornyshev, A.; Leikin, S. Fluctuation theory of hydration forces: the dramatic effects of inhomogeneous boundary conditions. *Phys. Rev. A* **1989**, *40*, 6431.

https://doi.org/10.1021/acs.nanolett.3c00927
Nano Lett. XXXX, XXX, XXX−XXX